International Journal of Control, Automation and Systems 14(1) (2016) 99-114
http://dx.doi.org/10.1007/s12555-014-0155-8
ISSN:1598-6446 eISSN:2005-4092
http://www.springer.com/12555

Adaptive Nonsingular Fast Terminal Sliding Mode Guidance Law with Impact Angle Constraints

Junhong Song, Shenmin Song*, and Huibo Zhou

Abstract: This paper considers the terminal guidance problem of missiles intercepting maneuvering targets with impact angle constraints. Based on an advanced nonsingular fast terminal sliding mode control scheme and adaptive control, an adaptive nonsingular fast terminal sliding mode guidance law is proposed in the presence of the target acceleration as an unknown bounded external disturbance. In the design procedure, an adaptive law is presented to estimate the unknown upper bound of the external disturbance. Theoretical analysis shows that the proposed guidance law can guarantee the finite-time convergence in both the reaching phase and the sliding phase by applying a Lyapunov-based approach. Numerical simulations are presented to demonstrate the effectiveness of the proposed guidance law. Although the proposed guidance law is developed for the constant speed missiles, by the extensive numerical simulations with a realistic missile model, the performance is shown to be equally good for the varying speed missiles.

Keywords: Adaptive control, finite-time convergence, guidance law, missile, terminal sliding mode.

NOMENCLATURE

a_m, a_t	lateral accelerations of the missile and target
r, $\dot{r}$	relative distance and relative velocity between the missile and target
V_m, V_t	velocities of the missile and target
q, $\dot{q}$	line-of-sight (LOS) angle and its rate
φ_m, φ_t	flight-path angles of the missile and target
t_f	guidance terminal time
φ_d	desired impact angle
q_d	desired terminal LOS angle
s	variable for the sliding surface
d	term of the lumped disturbance
Δ	unknown upper bound of the lumped disturbance
$\hat{\Delta}$	estimated value of Δ

1. INTRODUCTION

The main objectives of guidance laws are to allow missiles to intercept targets with minimum miss distances [1]. In order to increase the effectiveness of warheads against targets and achieve the best destroying effect, a specific impact angle needs to be considered. Therefore, it is necessary to make further study on the guidance law with terminal impact angle constraints, to meet the requirement of this special guidance mission. Proportional navigation (PN) guidance laws have been widely used to intercept targets with the impact angle constraints [2–4]. However, for the situation of intercepting the targets with a larger maneuverability, PN guidance laws are unable to intercept the targets under the required precision [5]. In order to deal with the maneuverable targets effectively, many researchers have developed various modern guidance laws, which are based on nonlinear H_∞ control [6], L_2 gain control [7], optimal control [8], differential game [9] and sliding mode control [10–16].

The sliding mode control (SMC) is well known for its good robustness to external disturbances and parametric uncertainties. The conventional linear sliding mode control (LSMC) [17], whose sliding mode manifold is a linear function, can only finish the asymptotic convergence in the sliding phase. In order to achieve the finite time convergence in the sliding phase, the terminal sliding mode control (TSMC), whose sliding mode manifold is a nonlinear function, is proposed in [18] for rigid robotic manipulators. In addition, the TSMC can provide faster convergence and higher precision control than the traditional LSMC. However, the initial TSMC results in two disadvantages. The first is the singularity problem. For exam-

Manuscript received April 16, 2014; revised October 9, 2014, and Febrary 3, 2015; accepted Febrary 10, 2015. Recommended by Associate Editor Chang Kyung Ryoo under the direction of Editor Duk-Sun Shim. This paper was supported by the Foundation for Creative Research Groups of the National Natural Science Foundation of China under Grant No.61021002.

Junhong Song, Shenmin Song, and Huibo Zhou are with the Center for Control Theory and Guidance Technology, Science Park of Harbin Institute of Technology, Yi Kuang Street, Nan Gang District, Harbin 150001, China (e-mails: hitsjh@163.com, songshenmin@hit.edu.cn, zhouhb0306@sina.com).
* Corresponding author.

ple, in the proposed guidance laws with the impact angle constraints in [12, 16], the TSMC algorithm was used to design the sliding mode surface. Because of the existing of the negative exponential term, the proposed guidance laws in [12,16] produced the singularity problem. In order to resolve the singularity problem, nonsingular terminal sliding mode controls (NTSMC) are developed in [19,20]. The NTSMC has been successfully used for the guidance law design with the impact angle constraints. For example, in [21, 22], nonsingular terminal sliding mode guidance laws with the impact angle constraints were proposed for the non-maneuvering targets. After that, NTSMC algorithm was also used to develop the guidance laws with the impact angle constraints to intercept the maneuvering target in [23, 24]. The second problem generated by the initial TSMC is that it has the slower convergence rate than the traditional LSMC when the system state is far away from the equilibrium. To overcome the second problem, fast terminal sliding mode controls (FTSMC) combining the advantages of LSMC and TSMC are given in [25,26]. However, the NTSMC in [19,20] and the FTSMC in [25, 26] can not solve the aforementioned both problems, simultaneously. In this paper, a nonsingular fast terminal sliding mode (NFTSM) is developed to not only avoid the singular problem but also improve the convergence rate when the system state is far away from the equilibrium, and based on the proposed NFTSM, a guidance law with the impact angle constraints is designed for the maneuvering target.

In the implementation of terminal sliding mode control, the switching gain selection is a difficult problem. As shown in [16,23], the implementation of the both proposed guidance laws needs to select the switching gain value, however, the information of the target acceleration affects the selection of the switching gain and is not easily obtained in many practical guidance processes. Generally speaking, in order to accomplish the sliding mode reaching condition, we should choose the switching gain larger than the upper bound of disturbance. So, a necessary assumption is that the disturbance is bounded and that its upper bound needs to be known in [10, 19]. However, in practical applications, the upper bound of disturbance is hard to know. To ensure that the guidance system has a good robustness, the enough large switching gain will be taken, which will produce a serious chattering problem. To resolve the above mentioned problem, the adaptive sliding mode control has been proposed in various literatures [27–34]. The important characteristic of the adaptive sliding mode control is that it adaptively tunes the switching gain by estimating the upper bound of the disturbance. So, a priori knowledge of the upper bound on the disturbance is not required to be known.

In this paper, the above-mentioned problems are addressed. Considering the target acceleration as unknown bounded external disturbance, the main contributions of this paper are stated as follows: (1) As compared with the existing TSMC approaches [18–20,25,26], an novel modified nonsingular fast terminal sliding mode (NFTSM) manifold is put forward. By use of the proposed NFTSM, both the above-mentioned problems generated by the initial TSMC are resolved. (2) Based on the proposed novel modified NFTSM manifold, an adaptive NFTSM guidance law with impact angle constraints for intercepting maneuvering targets is proposed. Compared with the existing TSM-based guidance law with impact angle constraints [12, 16], not only the proposed guidance law does not exhibit any singularity problem, but also the convergence rate of the system state is improved when the system state is far away from the equilibrium. In addition, by virtue of the use of adaptive control, the knowledge of the target acceleration is not required in advance. So, the proposed guidance law is robust to external disturbances with unknown bounds. (3) Compared with the existing adaptive sliding mode control approaches in [28–32] which can only guarantee the asymptotical stability, the proposed adaptive NFTSM guidance law can guarantee the finite-time convergences of the guidance system states in both the reaching phase and the sliding phase by a Lyapunov-based approach.

This paper is organized as follows. Some preliminaries are briefly stated in the following section. In Section 3, firstly, a new modified NFTSM manifold is given. Then, an adaptive NFTSM guidance law with impact angle constraints is proposed and the corresponding stability proofs are given as well. In Section 4, simulation results are presented, which are used to verify the effectiveness of the proposed guidance law. The last Section concludes this paper.

2. PROBLEM FORMULATION

This section presents the equations of guidance system for the missile intercepting the target. For simplicity, only a two-dimensional model is considered. The engagement geometry of a missile and a target is shown in Fig. 1, where the missile and the target are regarded as a point mass, respectively. We assume that the velocities of the missile and the target are constants, and the autopilot is fast enough to be neglected. Under these assumptions, the corresponding engagement dynamic equations can be described by the following differential equations:

$$\dot{r} = V_t \cos(q - \varphi_t) - V_m \cos(q - \varphi_m), \tag{1}$$

$$r\dot{q} = -V_t \sin(q - \varphi_t) + V_m \sin(q - \varphi_m), \tag{2}$$

$$\dot{\varphi}_t = a_t / V_t, \tag{3}$$

$$\dot{\varphi}_m = a_m / V_m, \tag{4}$$

where r and $\dot{r}$ denote the relative distance and the relative velocity from the missile to the target, respectively; V_t and V_m represent the velocities of the target and the missile,

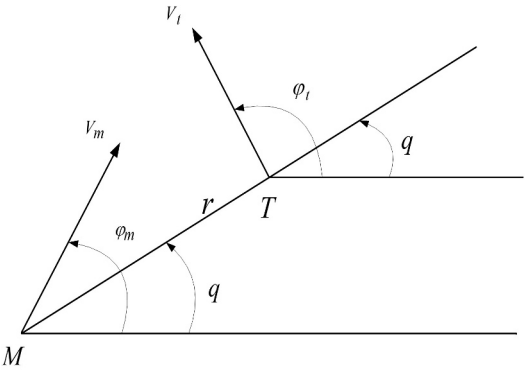

Fig. 1. Two-dimensional engagement geometry.

respectively; q and $\dot{q}$ denote the LOS angle and LOS angular rate between the missile and the target, respectively; φ_t and φ_m represent the flight-path angles of the target and the missile, respectively; a_m and a_t are the lateral accelerations of the missile and the target, respectively.

The impact angle is defined as the intersect angle between the velocity vectors of the missile and the target in the process of the missile intercepting the target. The guidance problem with impact angle constraint is to ensure that the missile hits the target with a desired impact angle, which means:

$$\lim_{t\to t_f} r(t)\dot{q}(t) = 0, \tag{5}$$

$$\varphi_m(t_f) - \varphi_t(t_f) = \varphi_d, \tag{6}$$

$$|\varphi_m(t_f) - q_d| < \pi/2, \tag{7}$$

wheret_f is the guidance terminal time, φ_d is the desired impact angle, and q_d is the desired terminal LOS angle. Equation (7) means that the target is in the vision scope when the missile hits it. From (2) and (5), we have

$$V_t \sin(\varphi_t(t_f) - q_d) - V_m \sin(\varphi_m(t_f) - q_d) = 0. \tag{8}$$

Then, it is very easy to obtain the following propositions.

Proposition 1 [35]**:** If $\varphi_t(t_f)$ is known, for a desired impact angle φ_d, $\varphi_m(t_f)$ can be obtained by applying (6). Then, there always exists a unique solution q_d for (7) and (8). Hence, the control problem of the impact angle can be transformed into the control problem of the terminal LOS angle, i.e., satisfying $q(t_f) = q_d$.

Proposition 2 [35]**:** Suppose $\varphi_t(t_f)$ and q_d are given. There exists a unique $\varphi_m(t_f)$ which satisfies the Eqs. (6)-(8).

Remark 1: When the target is stationary, then$\varphi_t(t_f) = 0$. When the target is non-maneuvering, $\varphi_t(t_f)$ is measurable. When the target is maneuvering, $\varphi_t(t_f)$ can be predicted by a tracking filter. Hence, we assume that the value of $\varphi_t(t_f)$ is known in the process of a guidance law design.

So, for a missile with a specific attack mission, the guidance problem with the impact angle constraints is converted to the control problem of terminal LOS angle satisfying $q(t_f) = q_d$, where q_d implies the desired terminal LOS angle to be a constant value [12,13,35–37].

By differentiating (2) with respect to time and using (1), (3) and (4), we can get

$$\ddot{q} = -\frac{2\dot{r}}{r}\dot{q} - \frac{\cos(q-\varphi_m)}{r}a_m + \frac{\cos(q-\varphi_t)}{r}a_t. \tag{9}$$

Note that, because the missile lateral acceleration a_m is multiplied by the term $\cos(q-\varphi_t)$, the LOS angle q can be controlled when $|q-\varphi_t| \neq \pi/2$. In [16], it have been proved that, if $|q-\varphi_t| = \pi/2$, then $\dot{q} - \dot{\varphi}_t \neq 0$. Therefore, $|q-\varphi_t| = \pi/2$ is not a stable equilibrium point and, as a result, the missile lateral acceleration a_m can be used to control the LOS angle q.

In this paper, required data such as $q, \dot{q}, r, \dot{r}$ and φ_m are available. Let q_d imply the desired terminal LOS angle and q_d is pre-specified with a constant value. Let q_e be the LOS angle error, i.e. $q_e = q - q_d$. Defining $x_1 = q_e = q - q_d$ and $x_2 = \dot{q}$. Substituting them into (9) yields

$$\begin{cases} \dot{x}_1 = x_2 \\ \dot{x}_2 = f + ba_m + d, \end{cases} \tag{10}$$

where

$$f = -\frac{2\dot{r}}{r}x_2, b = -\frac{\cos(q-\varphi_m)}{r}, d = \frac{\cos(q-\varphi_t)}{r}a_t.$$

Remark 2 [17]**:** Technically, the missile intercepting target by impact ("hit-to-kill") happens when $r \neq 0$ but belongs to the interval $r_0 \in [r_{\min}, r_{\max}] = [0.1, 0.25]m$.

Assumption 1: The target acceleration a_t is regarded as bounded external disturbance and satisfies $|a_t| \leq a_t^{\max}$, for all $t \geq 0$, with $a_t^{\max}$ a positive constant but unknown.

Assumption 2: In (10), d is regarded as an unknown lumped disturbance of target. From Assumption 1 and Remark 2, we can obtain that the following inequality holds

$$|d| = \left|\frac{\cos(q-\varphi_t)}{r}a_t\right| \leq \frac{a_t^{\max}}{r_0}. \tag{11}$$

So that, d is a bounded lumped external disturbance, i.e., $|d| \leq \Delta$, where Δ is an unknown positive constant.

This paper aims at developing a guidance law a_m such that the guidance law a_m can not only guarantee the missile has a small miss distance, but also guarantee the LOS angular rate and LOS angle error tend to a small enough neighborhood around zero in finite time in the presence of external disturbance and, as a result, quasi-parallel approach can be realized.

3. DESIGN OF THE ADAPTIVE NFTSM GUIDANCE LAW

3.1. Terminal sliding mode

The fast terminal sliding mode (FTSM) manifolds are proposed in [25] and [26], respectively, which can be described by the following equations:

$$s = \dot{y} + \alpha_1 y + \alpha_2 y^{p/q}, \tag{12}$$

$$s = \dot{y} + \alpha_1 y + \alpha_2 \mathrm{sig}(y)^{\gamma}, \tag{13}$$

where $\alpha_1, \alpha_2 > 0$, $0 < \gamma < 1$, $\mathrm{sig}(y)^{\gamma} = |y|^{\gamma}\mathrm{sign}(y)$, $q > p > 0$ are integers, q and p are odd.

The difference between (12) and (13) is that the range of the power γ is larger than that of the power p/q. Furthermore, the time derivatives of s defined by (12) and (13) are given as follows:

$$\dot{s} = \ddot{y} + \alpha_1 \dot{y} + \alpha_2 p/q y^{p/q-1}\dot{y}, \tag{14}$$

$$\dot{s} = \ddot{y} + \alpha_1 \dot{y} + \alpha_2 \gamma |y|^{\gamma^{-1}}\dot{y}. \tag{15}$$

By (14) and (15), we can discover that if $y = 0$ and $\dot{y} \neq 0$, the singularity will occur due to $p/q - 1 < 0$ and $\gamma - 1 < 0$. In order to avoid the singularity problem, a new form of nonsingular terminal sliding mode (NTSM) manifold in [20] is proposed, which can be described as follows:

$$s = \dot{y} + \alpha\beta(y), \tag{16}$$

where $\alpha > 0$ and $\beta(y) \in R$ is defined as

$$\beta(y) = \begin{cases} y^{p/q}, & \text{if } \bar{s} = 0 \text{ or } \bar{s} \neq 0, |y| > \eta \\ r_1 y + r_2 sign(y) y^2, & \text{if } \bar{s} \neq 0, |y| \leq \eta \end{cases}$$

with $\bar{s} = \dot{y} + \alpha y^{p/q}$, $r_1 = (2 - p/q)\eta^{p/q-1}$, $r_2 = (p/q - 1)\eta^{p/q-2}$, and η being a small positive constant.

Motivated by the work of [20], we define a novel modified NFTSM manifold which can be described by (17).

$$s = \dot{y} + \alpha_1 y + \alpha_2 \beta(y), \tag{17}$$

where α_1, $\alpha_2 > 0$ and $\beta(y) \in R$ is defined as

$$\beta(y) = \begin{cases} sig(y)^{\gamma}, & |y| > \eta \\ r_1 y + r_2 sign(y) y^2, & |y| \leq \eta \end{cases}$$

with $0 < \gamma < 1$, $r_1 = (2 - \gamma)\eta^{\gamma-1}$, $r_2 = (\gamma - 1)\eta^{\gamma-2}$, and η being a small positive constant. The time derivative of the proposed NFTSM manifold (17) can be written as:

$$\dot{s} = \begin{cases} \ddot{y} + \alpha_1 \dot{y} + \alpha_2 \gamma |y|^{\gamma-1}\dot{y}, & |y| > \eta, \\ \ddot{y} + \alpha_1 \dot{y} + \alpha_2 (r_1 \dot{y} + 2 r_2 y \dot{y} \mathrm{sign}(y)), & |y| \leq \eta. \end{cases}$$

Remark 3: The proposed NFTSM manifold$s$and its time derivative is continuous. Because the terminal sliding manifold is switched into the general sliding manifold in quadratic function form when y enters the region $|y| \leq \eta$, so the proposed sliding manifold can solve the singularity problem. In addition, the proposed sliding manifold can also improve the convergence rate when the system state is far away from the equilibrium point.

Based on the novel modified NFTSM manifold defined by (17), the NFTSM manifold$s$for the guidance system (10) is designed as follows:

$$s = x_2 + \alpha_1 x_1 + \alpha_2 \beta(x_1), \tag{18}$$

where α_1, $\alpha_2 > 0$ and $\beta(x_1) \in R$ is defined as

$$\beta(x_1) = \begin{cases} sig(x_1)^{\gamma}, & |x_1| > \eta \\ r_1 x_1 + r_2 \mathrm{sign}(x_1) x_1^2, & |x_1| \leq \eta \end{cases} \tag{19}$$

with $0 < \gamma < 1$, $r_1 = (2 - \gamma)\eta^{\gamma-1}$, $r_2 = (\gamma - 1)\eta^{\gamma-2}$, and η being a small positive constant.

3.2. Guidance law design

Now, we design the guidance law$a_m$for the guidance system (10) using the design principles of the sliding mode control. The first step is to develop a sliding mode manifold to obtain the desired control requirements. The sliding mode manifold is selected as the NFTSM manifold s (18).

Using (10), the time derivative of the NFTSM manifold s (18) can be written as

$$\dot{s} = f + b a_m + d + \alpha_1 x_2 + \alpha_2 \dot{\beta}(x_1). \tag{20}$$

To make the system trajectories fast converge to the designed NFTSM manifold s (18) from the initial states, a fast-TSM-type reaching law is selected in the form

$$\dot{s} = -k_2 s - k_1 \mathrm{sig}(s)^{\gamma_1}, \tag{21}$$

where $k_1, k_2 > 0$, $0 < \gamma_1 < 1$.

Substituting (20) into (21), we obtain the guidance law as follows:

$$a_m = \frac{-f - \alpha_1 x_2 - \alpha_2 \dot{\beta}(x_1) - d - k_1 \mathrm{sig}(s)^{\gamma_1} - k_2 s}{b}. \tag{22}$$

In practical guidance process, the lumped disturbance d which includes target acceleration may not be easily obtained. From the above-mentioned contents, we know that the lumped disturbance exists the upper bound which be estimated by an adaptive law. So the guidance law is modified into the following form:

$$a_m = \frac{-f - \alpha_1 x_2 - \alpha_2 \bar{\beta}(x_1) - \hat{\Delta}\sigma \mathrm{sign}(s) - k_1 \mathrm{sig}(s)^{\gamma_1} - k_2 s}{b}, \tag{23}$$

where $k_1, k_2 > 0$, $0 < \gamma_1 < 1$ and $\sigma \geq 1$ are designed constants, $\bar{\beta}(x_1)$ is the time derivative of the function $\beta(x_1)$ and has the following expression

$$\bar{\beta}(x_1) = \begin{cases} \gamma |x_1|^{\gamma-1} x_2, & |x_1| > \eta \\ r_1 x_2 + 2 r_2 x_1 x_2 \mathrm{sign}(x_1), & |x_1| \leq \eta \end{cases} \tag{24}$$

and $\hat{\Delta}$ is the estimate of Δ, which is given by the following adaptive law:

$$\dot{\hat{\Delta}} = \sigma |s| \quad (\hat{\Delta}(0) > 0). \tag{25}$$

To verify the finite time convergence of the guidance law (23), The following lemma is presented.

Lemma 1 [26]**:** Suppose that there exists a continuous positive definite function$V(t)$, and that $\dot{V}(t) \leq -\alpha V(t) - \beta V(t)^{\gamma}$, $\forall t > t_0$, where $\alpha > 0, \beta > 0$ and $0 < \gamma < 1$. Then, $V(t)$ converges to the equilibrium point in finite time t_f given by

$$t_f \leq t_0 + \frac{1}{\alpha(1-\gamma)} \ln \frac{\alpha V(t_0)^{1-\gamma} + \beta}{\beta}. \tag{26}$$

Then we obtain the following results.

Theorem 1: For the guidance system described by (10), if the NFTSM manifold is provided by (18), the guidance law is chosen as (23) and the adaptive law is designed as (25), then we conclude that $\tilde{\Delta}$ and s are all bounded.

Proof: We choose the following positive definite function as a Lyapunov function

$$V_1 = \frac{1}{2}s^2 + \frac{1}{2}\tilde{\Delta}^2, \tag{27}$$

where $\tilde{\Delta} = \Delta - \hat{\Delta}$ is the estimation error of Δ. Applying (10) , (18)and (23)-(25), the time derivative of V_1 can be written as:

$$\begin{aligned}
\dot{V}_1 &= s\dot{s} + \tilde{\Delta}\dot{\tilde{\Delta}} \\
&= s(d - \hat{\Delta}\sigma \text{sign}(s) - k_1 \text{sig}(s)^{\gamma_1} - k_2 s) - \sigma |s| (\Delta - \hat{\Delta}) \\
&= ds - \sigma |s| \Delta - k_1 |s|^{\gamma_1 + 1} - k_2 s^2 \\
&\leq \Delta |s| (1 - \sigma) - k_1 |s|^{\gamma_1 + 1} - k_2 s^2 \\
&\leq -k_1 |s|^{\gamma_1 + 1} - k_2 s^2 \leq 0.
\end{aligned} \tag{28}$$

It can be seen that $\dot{V}_1 \leq 0$. Thus $V_1(t) \leq V_2(0)$ holds, which implies that $V_1(t)$ is bounded. Hence, it can be concluded that the sliding mode variables s and $\tilde{\Delta}$ are all bounded. This completes the proof.

Remark 4: In Theorem 1, $\tilde{\Delta}$ and s do not converge to the regions near zero in finite time. It just guarantees that $\tilde{\Delta}$ and s have the bounds. Therefore, we put forward the next theorem which can guarantee that s converges to zero in finite time and x_1, x_2 converge to the regions near zero in finite time.

Theorem 2: Consider the guidance system equation (10) with the modified NFTSM manifold equation (18). Then applying the guidance law equation (23) and the adaptive law equation (25), the modified NFTSM manifold s converges to zero in finite time and then the states of the guidance system (10) will converge to the regions

$$|x_1| \leq \Delta_1 = \eta \tag{29}$$

$$|x_2| \leq \Delta_2 = \alpha_1 \eta + \alpha_2 \eta^{\gamma} \tag{30}$$

in finite time, respectively.

Proof: Consider the following positive definite function as a another Lyapunov function

$$V_2 = \frac{1}{2}s^2. \tag{31}$$

Using (10), (18) and (23)-(25), the time derivative of the Lyapunov function V_2 can be written as

$$\begin{aligned}
\dot{V}_2 &= s\dot{s} \\
&= s(d - \hat{\Delta}\sigma \text{sign}(s) - k_1 \text{sig}(s)^{\gamma_1} - k_2 s) \\
&= ds - \sigma\hat{\Delta}|s| - k_1 |s|^{\gamma_1 + 1} - k_2 s^2 \\
&\leq |s| (\Delta - \sigma\hat{\Delta}) - k_1 |s|^{\gamma_1 + 1} - k_2 s^2.
\end{aligned} \tag{32}$$

Since $\hat{\Delta}(0) > 0$ and $\dot{\hat{\Delta}} = \sigma |s| \geq 0$, there is $\hat{\Delta}(t) \geq \hat{\Delta}(0) > 0 (t \geq 0)$. Choose $\hat{\Delta}(0)$ large enough and σ satisfying

$$\sigma \geq \frac{\sqrt{s^2(0) + \hat{\Delta}^2(0)}}{\hat{\Delta}(0)} + 1. \tag{33}$$

Combining with $\hat{\Delta}(t) \geq \hat{\Delta}(0) > 0$, it can be obtained that

$$\begin{aligned}
\Delta - \hat{\Delta}\sigma &\leq \Delta - \sqrt{s^2(0) + \hat{\Delta}^2(0)} - \hat{\Delta}(0) \\
&= \tilde{\Delta}(0) - \sqrt{s^2(0) + \hat{\Delta}^2(0)} \\
&\leq |\tilde{\Delta}(0)| - \sqrt{s^2(0) + \hat{\Delta}^2(0)} \\
&= \sqrt{\tilde{\Delta}^2(0)} - \sqrt{s^2(0) + \hat{\Delta}^2(0)} \\
&\leq \sqrt{\hat{\Delta}^2(0)} - \sqrt{s^2(0) + \hat{\Delta}^2(0)} \\
&\leq 0.
\end{aligned} \tag{34}$$

From (34) we have

$$\begin{aligned}
\dot{V}_2 &\leq -k_1 |s|^{\gamma_1 + 1} - k_2 s^2 \\
&= -(\sqrt{2})^{\gamma_1 + 1} k_1 V_2^{\frac{\gamma_1 + 1}{2}} - 2k_2 V_2.
\end{aligned} \tag{35}$$

From (35) and according to Lemma1, the modified NFTSM manifold will converge to zero in finite time.

The stability analysis of the guidance system states convergence to the area near zero is as follows:

Case 1: If $|x_1| > \eta$, using (18), we obtain

$$s = x_2 + \alpha_1 x_1 + \alpha_2 \text{sig}(x_1)^{\gamma} = 0. \tag{36}$$

We select the Lyapunov function as $V_3 = \frac{1}{2}x_1^2$. Applying (10) and (36), the time derivative of the Lyapunov function

V_3 can be written as

$$\begin{aligned}\dot{V}_3 &= x_1\dot{x}_1 \\ &= x_1(-\alpha_1 x_1 - \alpha_2 \mathrm{sig}^{\gamma}(x_1)) \\ &= -2\alpha_1 V_3 - (\sqrt{2})^{\gamma+1}\alpha_2 V_3^{\frac{\gamma+1}{2}}.\end{aligned} \tag{37}$$

From (37) and according to Lemma 1, we have that the system state x_1 will converge to the region $|x_1| \le \eta = \Delta_1$ in finite time.

Furthermore, using (36), we obtain

$$\begin{aligned}|x_2| &\le \alpha_1 |x_1| + \alpha_2 |x_1|^{\gamma} \\ &\le \alpha_1 \eta + \alpha_2 \eta^{\gamma}.\end{aligned} \tag{38}$$

Therefore, the system state x_2 will converged to the region $|x_2| \le \alpha_1\eta + \alpha_2\eta^{\gamma} = \Delta_2$ in finite time.

Case 2: If $|x_1| \le \eta$, which implies that the system state x_1 has converged to the region $|x_1| \le \eta = \Delta_1$ in finite time, applying (18), then we obtain

$$s = x_2 + \alpha_1 x_1 + \alpha_2(r_1 x_1 + r_2 \mathrm{sign}(x_1)x_1^2) = 0. \tag{39}$$

From (39), we have the following inequality

$$\begin{aligned}|x_2| &\le \alpha_1 |x_1| + \alpha_2 \left|r_1 x_1 + r_2 \mathrm{sign}(x_1)x_1^2\right| \\ &\le \alpha_1 \eta + \alpha_2 \eta^{\gamma}.\end{aligned} \tag{40}$$

Therefore, according to (40), we conclude that the system state x_2 will converge to the region $|x_2| \le \alpha_1\eta + \alpha_2\eta^{\gamma} = \Delta_2$ in finite time. This completes the proof.

Remark 5: From (29) and (30), it is concluded that the higher the convergence accuracy of x_1 and x_2, the smaller the guidance law parameter η is required. In addition, from (19), we can see that the selection of η value affects the effectiveness of the dealing with the singularity problem. That is, the bigger the value of $|x_1|^{\gamma-1}x_2$, the smaller the guidance law parameter η is selected. Such as, when η=0, the proposed sliding mode surface (18) changes into the general fast terminal sliding mode which results in the singularity problem. In order to consider the singularity problem and the convergence precision of system states simultaneously, we can eclectically choose η according to the control requirements of the system. From (30), it is obtained that the guidance law parameter α_1, α_2 and γ determine the convergence accuracy of the LOS angular rate x_2. The smaller LOS angular rate x_2, the smaller guidance law parameters α_1, α_2 and $1/\gamma$ are required.

Because of the discontinuous signum function $\mathrm{sign}(s)$ in (23), the adaptive NFTSM guidance law is a discontinuous controller which can induce the chattering problem. In order to remove the chattering, the signum function $\mathrm{sign}(s)$ is replaced with a continuous sigmoid function

$$\mathrm{sgmf}(s) = \begin{cases} \mathrm{sign}(s), & |s| > \delta \\ 2\left(\frac{1}{1+\exp^{-as}} - \frac{1}{2}\right), & |s| \le \delta, \end{cases} \tag{41}$$

where δ is a small positive constant and a is a constant that is inversely proportional to δ.

Hence, the adaptive NFTSM guidance law in (23) is modified as

$$a_m = \frac{-f - \alpha_1 x_2 - \alpha_2 \bar{\beta}(x_1) - \hat{\Delta}\sigma\,\mathrm{sgmf}(s) - k_1 \mathrm{sig}(s)^{\gamma_1} - k_2 s}{b}. \tag{42}$$

4. SIMULATION RRESULTS

In this section, a missile is considered in its terminal guidance process to intercept a maneuvering target. Next simulations are conducted for different kinds of scenarios to illustrate the effectiveness of the proposed guidance law (42). The initial conditions for the missile and the target are shown in Table 1.

In guidance law (42), the parameters are chosen as $\alpha_1 = 0.5$, $\alpha_2 = 0.5$, $\gamma = 2/3$, $\sigma = 1.1$, $k_1 = 6$, $k_2 = 2$, $\gamma_1 = 9/10$, $\eta = 0.001$, $a = 1/\delta$ and $\delta = 0.002$. The maximum acceleration of the missile is $40g$, g is the acceleration of gravity ($g = 9.8\ m/s^2$).

4.1. Constant speed missiles

In the subsection, the simulation results for the constant speed missiles are presented.

The first set of simulations for the missile intercepting different kinds of targets at the desired terminal LOS angle of 20deg ($q_d = 20\mathrm{deg}$) are presented. The initial conditions of missile and target are selected as the data set 1 in Table 1. In order to verify the effectiveness of the proposed guidance law, three different target acceleration profiles, which are cosine maneuvering, step maneuvering and constant maneuvering, are considered as given below.

1) Case1. $a_t = 7g\cos(\pi t/4)m/s^2$.

2) Case2. $a_t = 7gm/s^2$ for $t < 5s$ and $a_t = -7gm/s^2$ for $t \ge 5s$.

3) Case3. $a_t = 7g\ m/s^2$.

With the proposed guidance law (42), simulations are performed for the target acceleration profiles of case 1 to case 3. Simulation results obtained are shown in Figs. 2-7 and Table 2, respectively. Figs. 2-7 show the curves of trajectories of the missile and the target, LOS angle error,

Table 1. The initial conditions for the missile and target.

Initial condition	Data set 1	Data set 2
$x_m(0)$	0m	0km
$y_m(0)$	0m	16km
$\varphi_m(0)$	60deg	50deg
V_m	600m/s	1032.7m/s
$x_t(0)$	$2500\sqrt{3}$m	1km
$y_t(0)$	2500m	16.4km
$\varphi_t(0)$	0deg	60deg
V_t	300m/s	900m/s

LOS angular rate, sliding mode manifold, missile acceleration command and adaptive parameter $\hat{\Delta}$, respectively. Table 2 summarizes the miss distances and LOS angle errors from the target acceleration profiles of case 1 to case 3.

The trajectories of the missile and the target for the cases 1-3 are shown in Fig. 2, which demonstrate that the proposed guidance law can ensure that the missile intercepts the target in any of the three cases successfully. From Fig. 3, we can observer that the proposed guidance law can guarantee the LOS angle errors converge to the neighbourhood of zero rapidly in finite time (in approximately 5s) for the target acceleration profiles of case 1 to case 3. That is to say, Fig. 3 shows that the proposed guidance law can ensure that the missile intercepts the target with the desired terminal LOS angle 20deg in any of the three cases successfully. Fig. 4 indicates that,

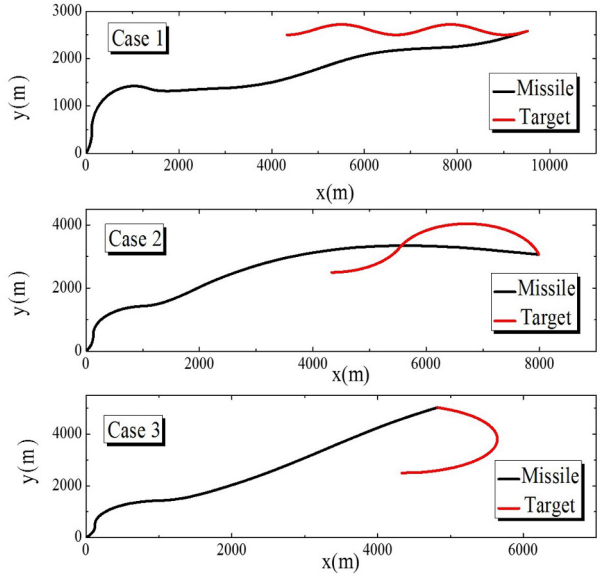

Fig. 2. Trajectories of missile and target.

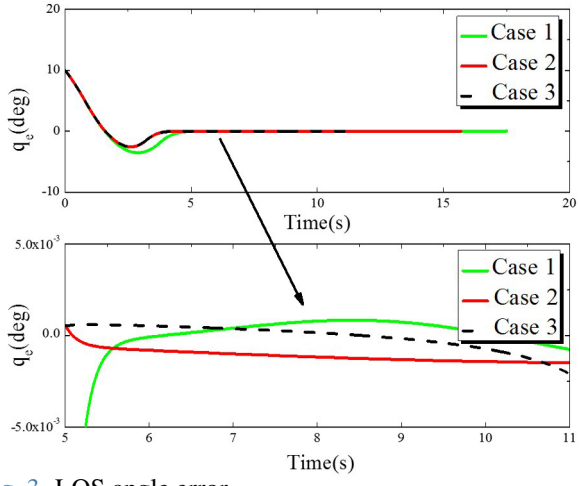

Fig. 3. LOS angle error.

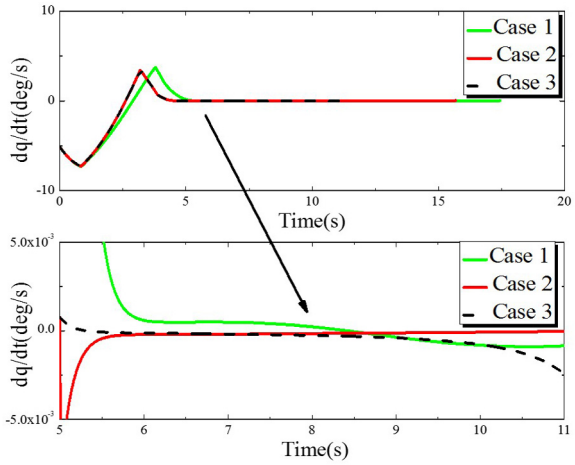

Fig. 4. LOS angular rate.

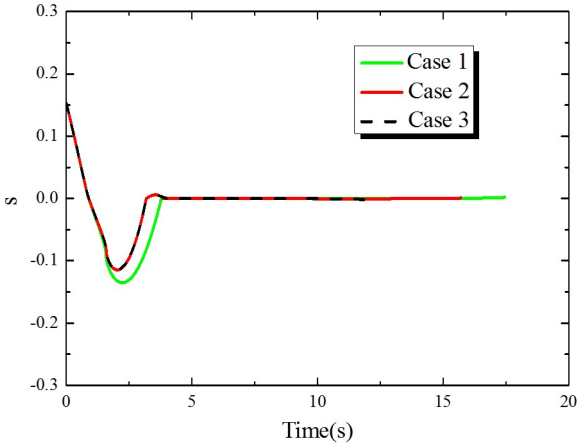

Fig. 5. Sliding mode manifold.

under the proposed guidance law, the LOS angular rates can also converge to the neighbourhood of zero rapidly in finite time (in approximately 5s) for the cases 1-3 and the convergence error is less than 0.005 deg/s after 5 seconds. In addition, for any case we can see that the curve of the LOS angular rate has peaks in first 5 seconds of the guidance process, which leads to the requirement of needing relatively large missile acceleration shown in Fig. 6. However, the relatively large missile acceleration can guide the LOS angular rate to the neighbourhood of zero rapidly. And the missile acceleration is decreasing correspondingly as the LOS angular rates tend to zero. It can be seen from Fig. 5 that the sliding mode manifolds converge to zero fast in finite time under the proposed guidance law for the target acceleration profiles of case 1 to case 3. As shown in Fig. 6, it can be observed that the missile lateral accelerations are within the reasonable bounds and there are acceleration saturations problem before 5s in all the three cases. But, the missile lateral accelerations are decreasing correspondingly until tending to zero as the LOS angular rate converges to the neighbourhood around

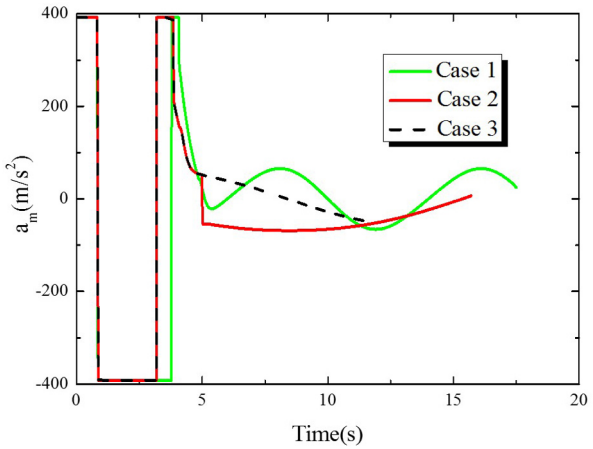

Fig. 6. Missile acceleration.

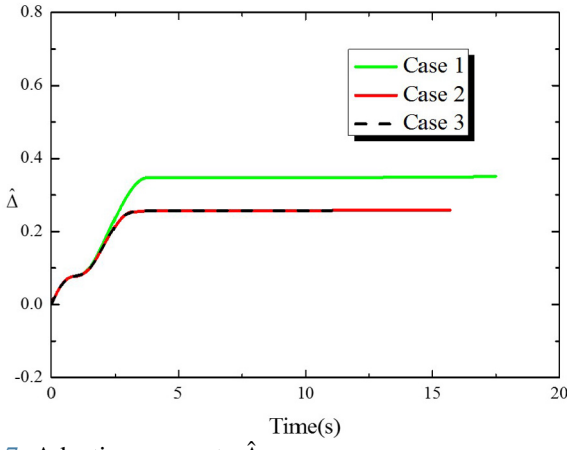

Fig. 7. Adaptive parameter$\hat{\Delta}$.

Table 2. Miss distances and LOS angle errors of three cases.

Target acceleration profile	Miss distance(m)	LOS angle error(deg)
Case 1	0.025	0.019
Case 2	0.158	0.003
Case 3	0.160	-0.012

zero. From Fig. 7, it can be seen that the upper bound of lumped disturbance can be estimated fast for the target acceleration profiles of case 1 to case 3. And these adaptive parameters can converge to a small constant fast in finite time.

It can be noted from Table 2 that the proposed guidance law has small miss distances belonging to $[0.1, 0.25]$ and very small LOS angle errors for the three cases of target acceleration, which mean that the missile can intercept the maneuvering target with the desired terminal LOS angle by hit-to-kill guidance strategy.

The next simulations for the guidance laws based on different forms of sliding mode are shown. In order to verify the effectiveness of the proposed NFTSM in this paper, the LSM and the initial TSM is used to design the guidance laws under the same conditions next. For comparison, the LSM manifold$s$is defined as

$$s = x_2 + (\alpha_1 + \alpha_2)x_1 \tag{43}$$

and the LSM guidance law is given by

$$a_m = \frac{-f - (\alpha_1 + \alpha_2)x_2 - \hat{\Delta}\sigma\mathrm{sgmf}(s) - k_1\mathrm{sig}(s)^{\gamma_1} - k_2 s}{b}. \tag{44}$$

The TSM manifold s is defined as

$$s = x_2 + (\alpha_1 + \alpha_2)sig(x_1)^{\gamma} \tag{45}$$

and the TSM guidance law is given by

$$a_m = 1/b[-f - (\alpha_1 + \alpha_2)\gamma|x_1|^{\gamma-1}x_2 - \hat{\Delta}\sigma\mathrm{sgmf}(s) - k_1\mathrm{sig}(s)^{\gamma_1} - k_2 s]. \tag{46}$$

All parameters of the LSM guidance law and TSM guidance law are chosen as the same as those given in the proposed guidance law. The initial conditions of missile and target and the desired terminal LOS angle constraints ($q_d = 20$deg) are the same as the previous simulation. The target acceleration is chosen as cosine maneuvering $a_t = 7g\cos(\pi t/4)m/s^2$, which is the same as Case 1. The response of the trajectories of the missile and the target, LOS angle error, LOS angular rate and missile acceleration command for the three kinds of guidance law are shown in Figs. 8 to 13. The interception times and miss distances for the considered guidance laws are shown in Table 3.

Note: The abbreviations in Figs. 8 to 13, i.e., NFTSM, LSM and TSM, denote the proposed adaptive NFTSM guidance law (42), the LSM guidance law (44) and the TSM guidance law (46). In Table 3, the abbreviations have the same meanings.

As shown in Fig. 8, it can be seen that the three kinds of guidance laws can accomplish the interception successfully. In addition, the proposed adaptive NFTSM guidance law guarantees the missile has shorter trajectories than that of the TSM guidance law. From the Figs. 9 and 10, it can be observed that the convergence rates of the LOS angle error and LOS angular rate under the proposed guidance law are similar to that under the LSM guidance law, respectively. However, the proposed guidance law can provide higher convergence precision than the LSM guidance law. From Figs. 11 and 12, it can be seen that the convergence precisions of the LOS angle error and LOS angular rate under the proposed guidance law are similar to that under the TSM guidance law. However, it can be seen clearly that the proposed guidance law has shorter convergence time than the TSM guidance law. From Fig. 13, we can observe that, during the initial process there are acceleration saturations problem under all the three guidance laws. However, under the TSM guidance law, there

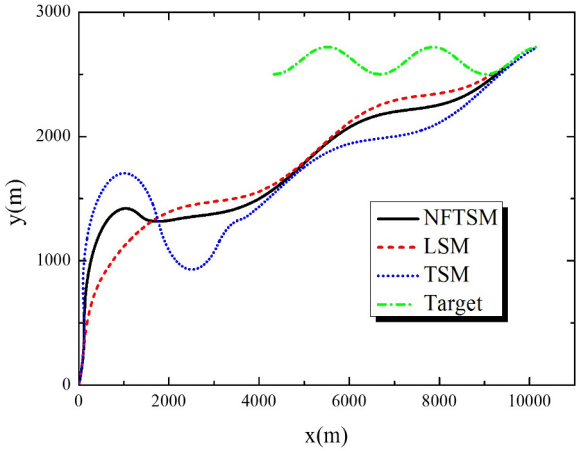

Fig. 8. Trajectories of missile and target.

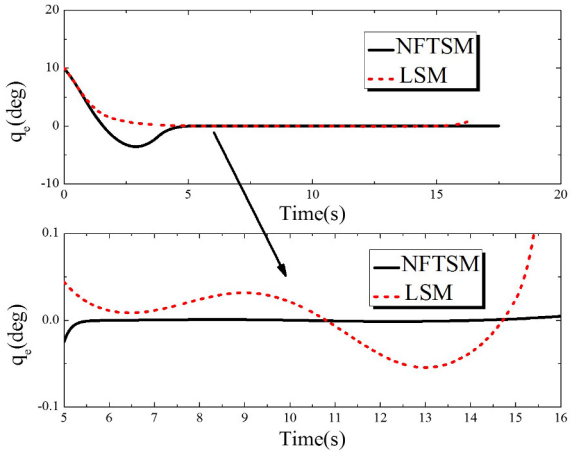

Fig. 9. LOS angle error between NFTSM and LSM.

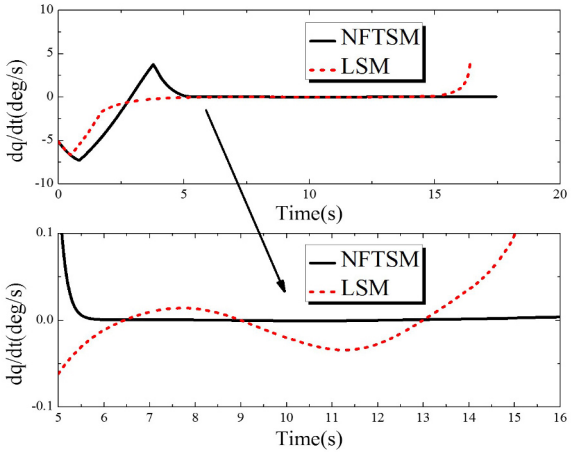

Fig. 10. LOS angular rate between NFTSM and LSM.

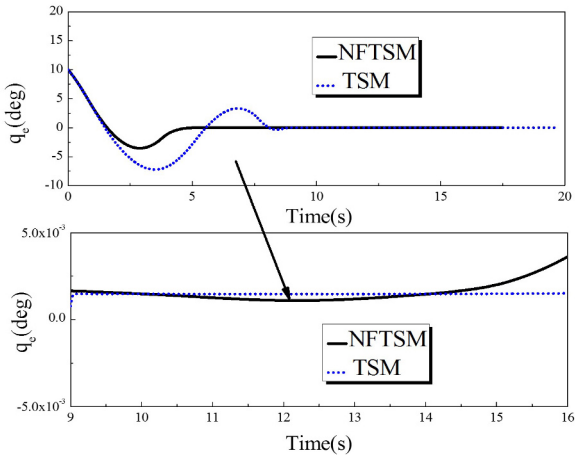

Fig. 11. LOS angle error between NFTSM and TSM.

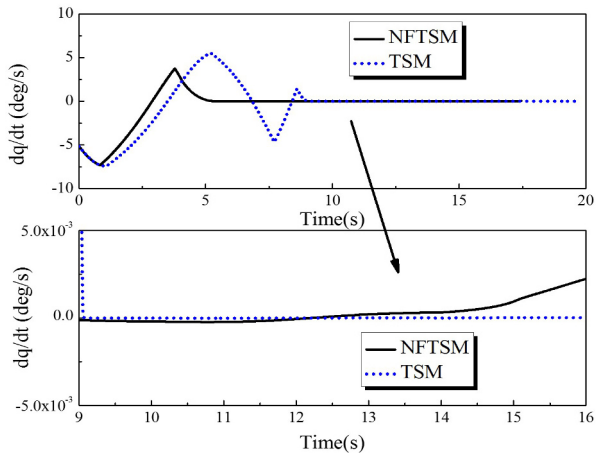

Fig. 12. LOS angular rate between NFTSM and TSM.

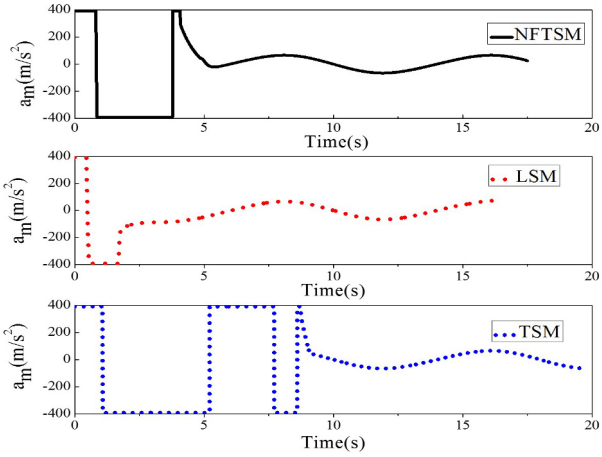

Fig. 13. Missile acceleration command.

is a longest time of acceleration saturation. Based on the above analysis, the performance of the proposed guidance law is superior to those of the LSM guidance law and TSM guidance law.

From Table 3, it is clear that the interception time taken by the adaptive NFTSM guidance law is similar to that of the LSM guidance law. However the TSM guidance law has longer interception time than the other guidance law. The miss distance generated by the NFTSM is smaller than the other guidance laws. So, the proposed adaptive

Table 3. Miss distances and interception times of three guidance laws.

Guidance law	Interception time(s)	Miss distance(m)
NFTSM	17.662	0.025
LSM	16.558	0.351
TSM	19.887	0.146

NFTSM guidance law is available to intercept the maneuvering target with the higher guidance precision.

The next set of simulations for the comparison between the proposed adaptive NFTSM guidance law and the similar guidance law existing in the literature [23] are presented. In [23], the guidance law is designed as

$$s = q_e + \beta(\dot{q}_e)\alpha \tag{47}$$

$$a_m = \frac{|\dot{r}|\dot{q}}{|\cos(q-\varphi_m)|}\left[2+\frac{r\dot{q}^{1-\alpha}}{\alpha\beta|\dot{r}|}\right] + \frac{M}{sign(\cos(q-\varphi_m))}\mathrm{sgmf}(s) \tag{48}$$

where

$$\mathrm{sgmf}(s) = \begin{cases} 2\left(\frac{1}{1+\exp^{-as}}-\frac{1}{2}\right), & |s|\le\varepsilon \\ \mathrm{sign}(s), & |s|>\varepsilon \end{cases} \tag{49}$$

Parameters are $\alpha = 5/3$, $\beta = 1$, $M = 3\times10^3$, $a = 1/\varepsilon = 20$.

For simplicity, we denote the proposed guidance law in this paper and the guidance law in the literature [23] as NFTSM guidance law and NTSM guidance law respectively.

The initial conditions of missile and target and the desired terminal LOS angle constraints ($q_d = 20$ deg) are the same as the previous simulation. The target acceleration is chosen as cosine maneuvering $a_t = 7g\cos(\pi t/4)m/s^2$. The simulation cures including the trajectories of missile and target, the LOS angle error, the LOS angular rate and missile acceleration command for the both guidance laws are shown in Figs. 14 to 17. The interception times, miss distances and LOS angle errors for the considered guidance laws are shown in Table 4.

From Fig. 14, it can be observed that the proposed adaptive NFTSM guidance law has shorter trajectories than that of the NTSM guidance law, which can also be seen from the interception time listed in Table 4. Under the proposed adaptive NFTSM guidance law the intercepting time is 17.662 seconds, but, the intercepting time for the NTSM guidance law is 38.800 seconds. From Fig. 15, we can observer that the proposed adaptive NFTSM guidance law can guarantee the LOS angle error converges to the neighbourhood of zero rapidly in finite time (in approximately 5s). However, under the NTSM guidance law the convergence rate of the LOS angle error is much slower than that under the proposed adaptive NFTSM guidance law. The LOS angle error under the NTSM guidance law

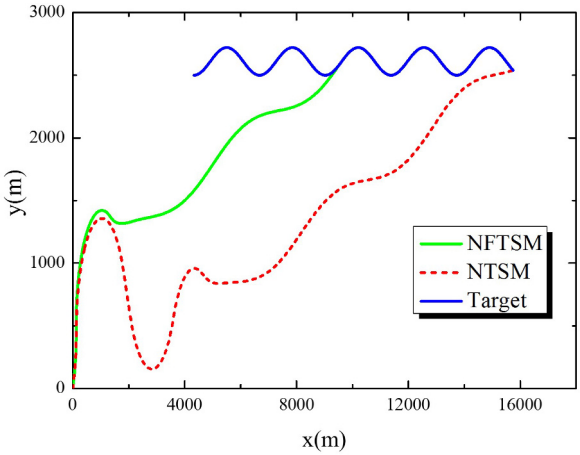

Fig. 14. Trajectories of missile and target.

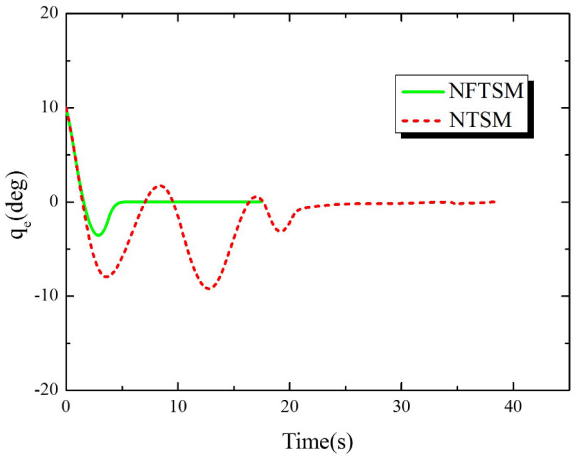

Fig. 15. LOS angle error.

converges to the neighbourhood of zero in approximately 25 seconds. In addition, from the LOS angle error listed in Table 4, it can be seen that the LOS angle error under the proposed adaptive NFTSM guidance law is 0.019deg, which is less than that 0.05deg under the NTSM guidance law. As shown in Fig. 16, it can be also observed that the convergence rate of the LOS angular rate under the NFTSM guidance law is much faster than that of the NTSM guidance law. And, the LOS angular rate under the NTSM guidance law appears the chattering phenomenon at about $t = 35$ sec. Fig. 17 demonstrates that the missile applies a larger later acceleration during the start of the guidance process for the both NFTSM guidance law and NTSM guidance law. However, these large demands on the lateral missile acceleration can guarantee that the LOS angle and the LOS angular rate converge to their corresponding desired values in finite time. That is, we can also see that the missile lateral accelerations are decreasing correspondingly until tending to zero as the LOS angular rate converges to the neighbourhood around zero. In addition, the missile acceleration under the NTSM guidance law appears the chattering phenomenon at about $t = 35$ sec. So, the NFTSM guidance law has better guidance

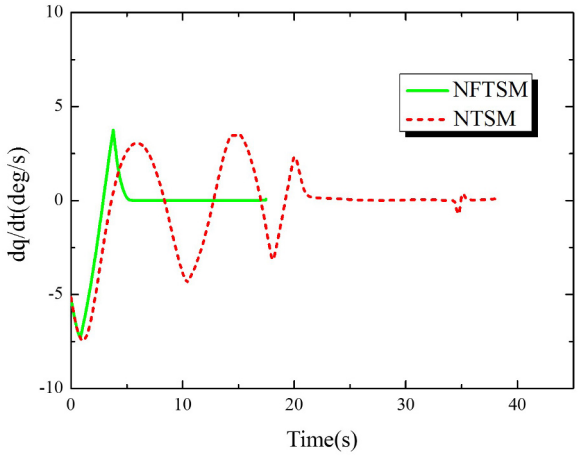

Fig. 16. LOS angular rate.

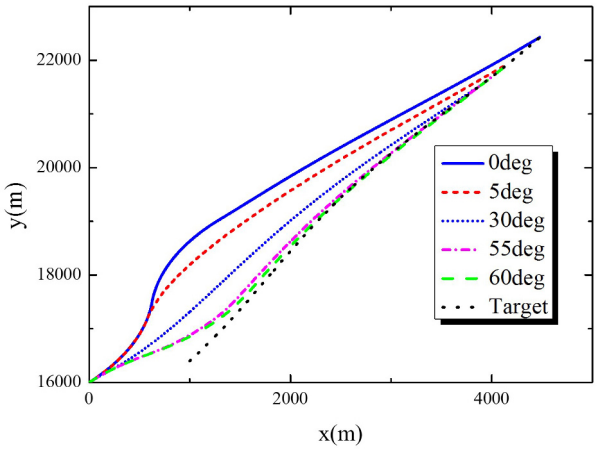

Fig. 18. Trajectories of missile and target.

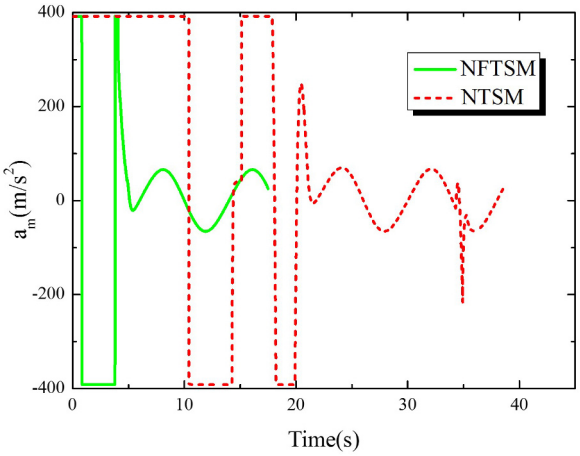

Fig. 17. Missile acceleration command.

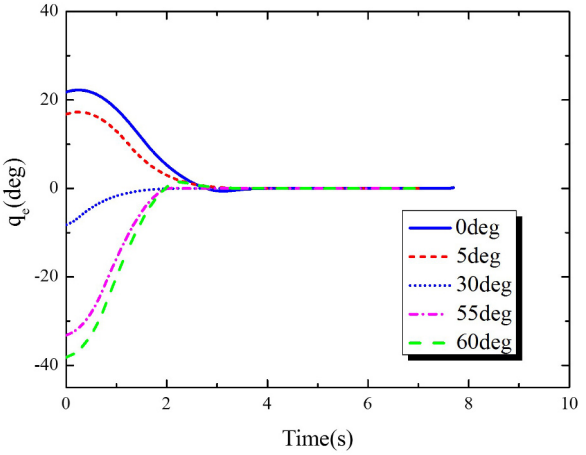

Fig. 19. LOS angle error.

Table 4. Interception times, miss distances and LOS angle error of the both guidance laws.

Guidance law	Interception time(s)	Miss distance(m)	LOS angle error(deg)
NFTSM	17.662	0.025	0.019
NTSM	38.800	0.110	0.050

performance than the NTSM guidance law.

From Table 4, the proposed adaptive NFTSM guidance law can ensure the missile has much smaller miss disturbance and LOS angle error than that of the NTSM guidance law. Then, the guidance precision of the NFTSM guidance law is significantly superior to that of the NTSM guidance law.

All of the previous simulations are done only for a specific desired terminal LOS angle as well as the initial flight path angle of the missile. In order to validate the proposed adaptive NFTSM guidance law, the next simulation for different desired terminal LOS angles but from the same initial flight path angle of the missile are shown. The initial conditions of missile and target are selected as the data set 2 in Table 1. Let the desired terminal LOS angles be 0 deg, 5 deg, 30 deg, 55 deg, 60 deg respectively. The target acceleration is also chosen as cosine maneuvering $a_t = 7g\cos(\pi t/4)m/s^2$. With the implement of the proposed adaptive NFTSM guidance law, the trajectories of missile and target, the LOS angle error, the LOS angular rate and missile acceleration command for these cases are given in Figs. 18 to 21. The miss distances and the LOS angle errors are shown in Table 5.

From Fig. 18, it can be seen that the missile can intercept precisely the target for the different desired terminal LOS angles. Figs. 19–21 show that, when $q_d = 5°$, $30°$, $55°$, the LOS angle errors and the LOS angular rates can converge rapidly to the neighbourhood of zero in finite time and the missile accelerations are within the reasonable bounds. However, when $q_d = 0°$, $60°$, the missile accelerations have a sudden rise toward interception. Therefore, the LOS angular rates are divergent in the end of guidance which causes the large miss distance given in Table 5. From Table 5, it can be observed that the miss distances and the LOS angle error for $q_d = 5°$, $30°$, $55°$ are much smaller than that for $q_d = 0°$, $60°$. So, the optimal desired LOS angle of the proposed adaptive NFTSM

guidance law approaches $q_d = [5°, 55°]$. The proposed guidance law in this paper can make missile hit precisely maneuvering target for arbitrary given desired LOS angle in this interval $[5°, 55°]$.

A final simulation for different initial flight path angles of the missile but from the same desired terminal LOS angle are performed with the proposed NFTSM guidance law. In this case, a desired terminal LOS angle of 50 deg ($q_d = 50$ deg) is desired. The missile's initial flight path angles are selected as 30 deg, 45 deg, 60 deg respectively. The other initial conditions of missile and target are selected as the data set 2 in Table 4. The target acceleration is chosen as cosine maneuvering $a_t = 7g\cos(\pi t/4)\ m/s^2$. Figs. 22–25 show the results from the simulation for these cases. The trajectories of missile and target for each initial flight path angle are shown in Fig. 22. From Fig. 22, it can be seen that the proposed adaptive NFTSM guidance law can guarantee that the missile intercepts the maneuvering target successfully at the desired terminal LOS angle for the respective selected initial flight path angles. Figs. 23-24 show that each of the LOS angle errors and the LOS angular rates can converge to the neighbourhood of zero fast in finite time from the respective given initial flight path angles. Fig. 25 depicts the missile acceleration commands for the three kinds of initial flight path angles. It can be observed that the missile accelerations are within the reasonable bounds and there are acceleration saturations problem before 2s in all the three cases. But, the missile accelerations approach zero fast and become smooth after 2s.

The miss distances and the LOS angle errors for these given initial flight path angles are given in Table 6. From the Table it can be noted that the proposed adaptive NFTSM guidance law has small miss distances and the LOS angle errors for the different given initial flight path angles, which means that the missile which mean that the missile can impact precisely the maneuvering target with the desired terminal LOS angle.

4.2. Realistic missiles

In the above subsection, only the simulation results for the constant speed missiles are shown. Nonetheless, as we all know, the speed of the missile for a realistic missile model is variable, hence, the following simulation results will be presented to demonstrate the effectiveness of the proposed guidance law in this paper for missiles with varying speed which is as good as that for the constant speed missiles. This is due to the inherently strong robustness of the designed guidance law. For simplicity, only a two-dimensional model is considered to design the guidance law in this paper. So, a realistic missile model [23] in the pitch plane is used to validate the effectiveness of the designed guidance law.

The equations of motion of a point-mass flying over a

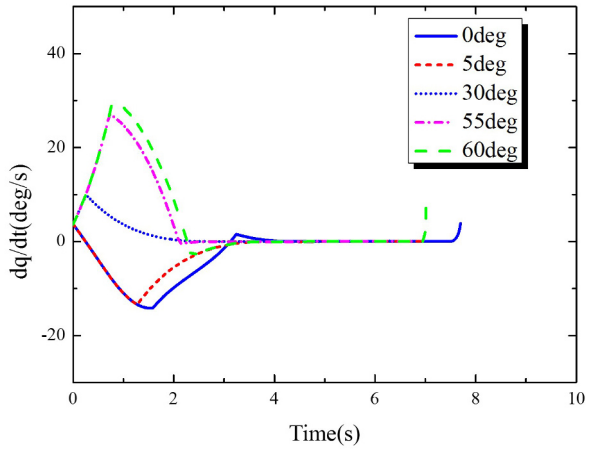

Fig. 20. LOS angular rate.

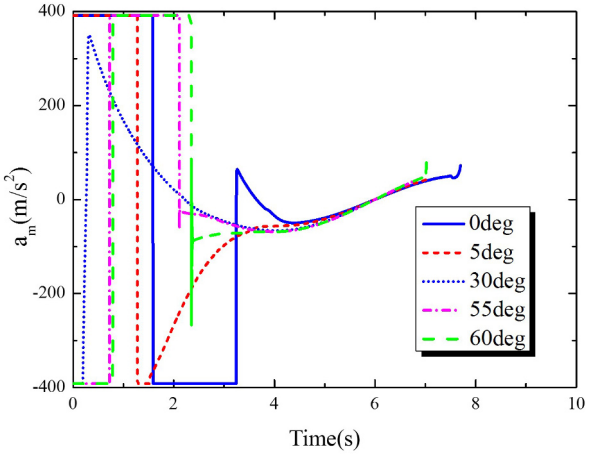

Fig. 21. Missile acceleration command.

Table 5. Miss distances and LOS angle error for the different desired terminal LOS angles.

Desired terminal LOS angle	Miss distance(m)	LOS angle error(deg)
0 deg	0.280	0.207
5 deg	0.089	0.008
30 deg	0.004	0.021
55 deg	0.058	0.007
60 deg	0.331	0.252

flat, non-rotating Earth are given by

$$\dot{x}_m = V_m \cos\varphi_m \tag{50}$$

$$\dot{y}_m = V_m \sin\varphi_m \tag{51}$$

$$\dot{V}_m = \frac{T-D}{m} - g\sin\varphi_m \tag{52}$$

$$\dot{\varphi}_m = \frac{a_m - g\cos\varphi_m}{V_m}, \tag{53}$$

where x_m and y_m are the position of the missile; m,V_m and φ_m represent the mass, the velocity and the flight path angle of the missile, respectively; T and D denote the thrust

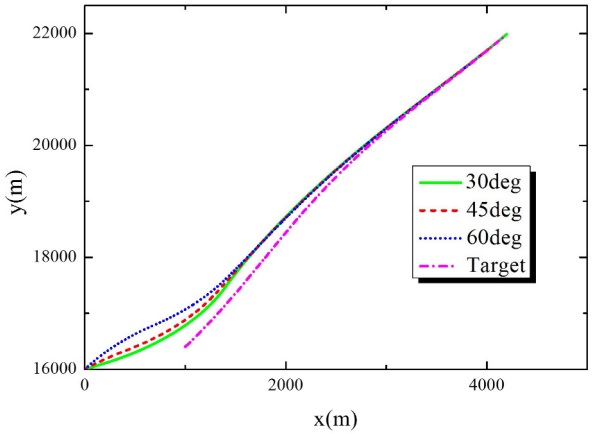

Fig. 22. Trajectories of missile and target.

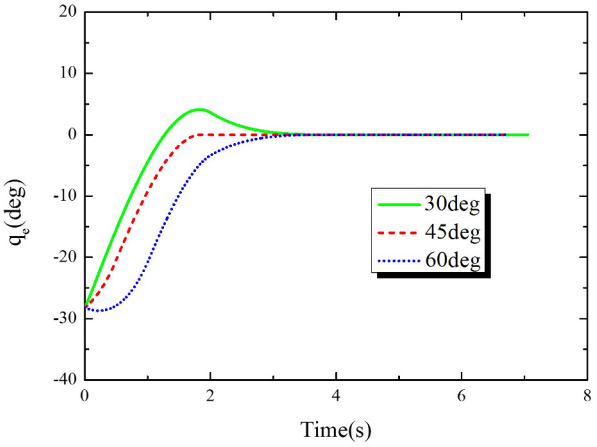

Fig. 23. LOS angle error.

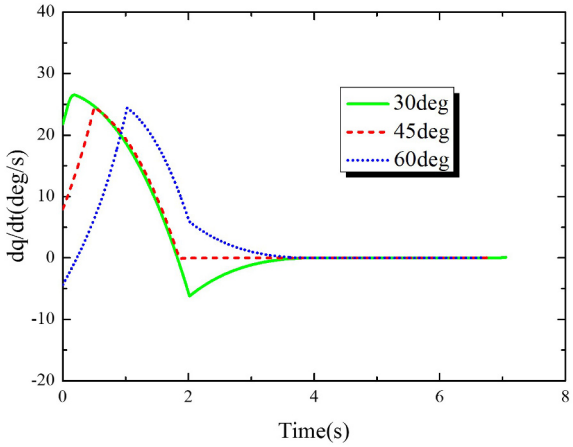

Fig. 24. LOS angular rate.

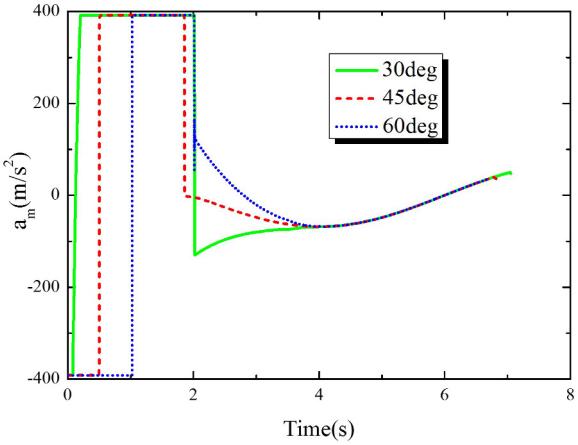

Fig. 25. Missile acceleration command.

and the drag of the missile, respectively; g denotes the acceleration due to gravity, and a_m is the lateral acceleration of the missile.

For the realistic missile model, the aerodynamic drag D in (52) is modeled as

$$D = D_0 + D_i;\ \ D_0 = C_{D0}Qs;\ \ D_i = \frac{Km^2a_m^2}{Qs};$$
$$K = \frac{1}{\pi A_r e};\ \ Q = \frac{1}{2}\rho V_m^2 \tag{54}$$

where D_0 and D_i are the zero-lift drag and induced drag; C_{D0} and K denote the zero-lift drag coefficient and the induced drag coefficient; Q, A_r, e, s and ρ represent the dynamic pressure, the aspect ratio, the efficiency factor, reference area and the atmosphere density, respectively. For these (50)-(54), the realistic missile parameters used in simulation are given the same as that in [23].

The initial conditions of missile and target are selected as the data set 1 in Table 1. The desired terminal LOS angle q_d is pre-specified to be 20 deg. The target acceleration is also chosen as cosine maneuvering $a_t = 7g\cos(\pi t/4)m/s^2$. With the implement of the proposed adaptive NFTSM guidance law (42), the trajectories of missile and target, the

Table 6. Miss distances and LOS angle errors for the different initial flight path angles.

Initial flight path angle	Miss distance(m)	LOS angle error(deg)
30 deg	0.012	0.009
45 deg	0.050	0.015
60 deg	0.011	0.007

LOS angle error, the LOS angular rate, sliding mode manifold, missile acceleration com mand and variation of the missile speed are given in Figs. 26 to 31.

The trajectories of the missile and the target are shown in Fig. 26, which demonstrate that the proposed guidance law can ensure that the realistic missile intercepts the maneuvering target successfully. Figs. 27–30 can be compared with the Case 1 of the Figs. 3–6. It can be seen that, under the proposed guidance law, the curves of the LOS angle error, the LOS angular rate, the sliding mode manifold and the missile acceleration command for the varying speed missile have similar trends as those for the constant speed missile, respectively. From Fig. 31, it can be observed that the speed of the missile fast increases at the start of the engagement owing to the larger thrust com-

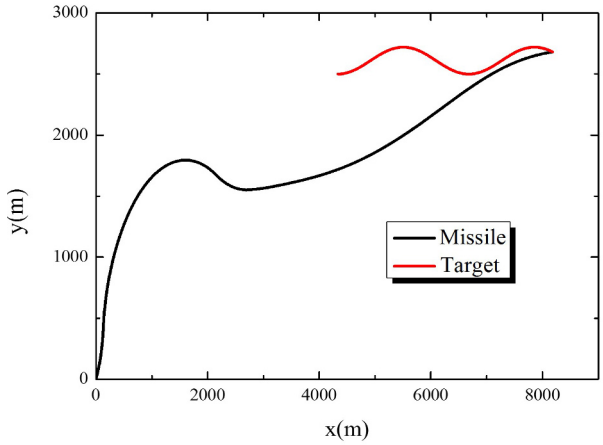

Fig. 26. Trajectories of missile and target.

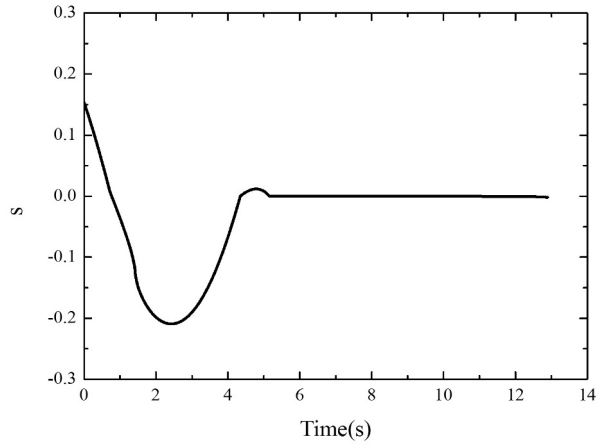

Fig. 29. Sliding mode manifold.

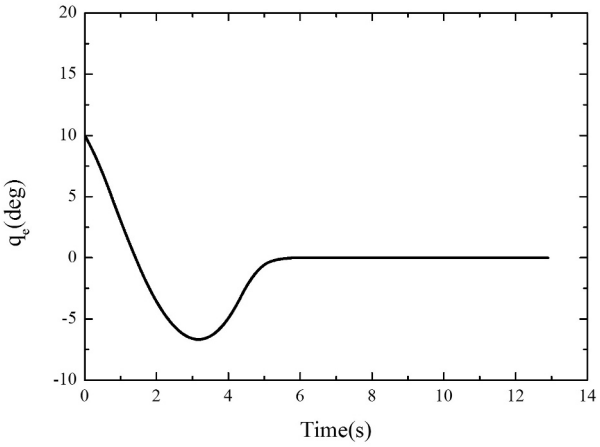

Fig. 27. LOS angle error.

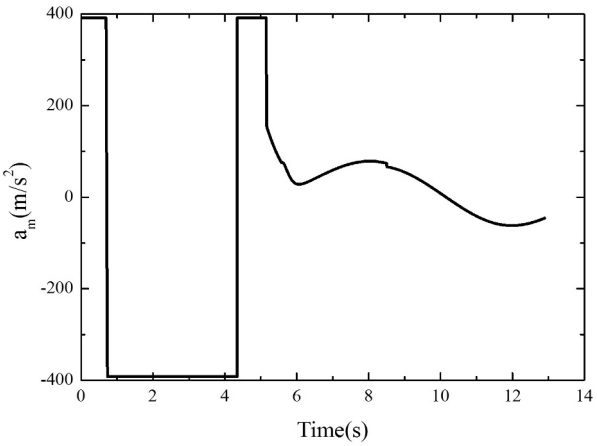

Fig. 30. Missile acceleration command.

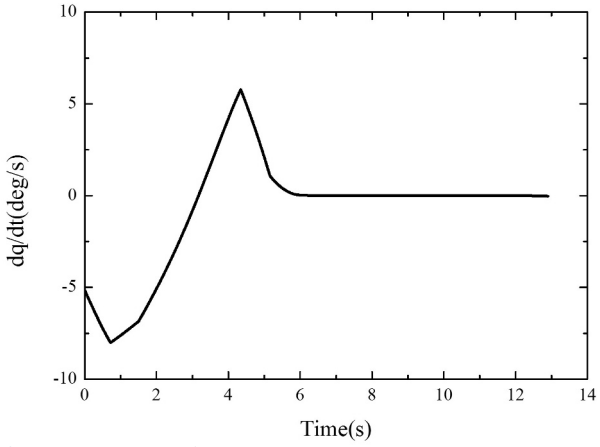

Fig. 28. LOS angular rate.

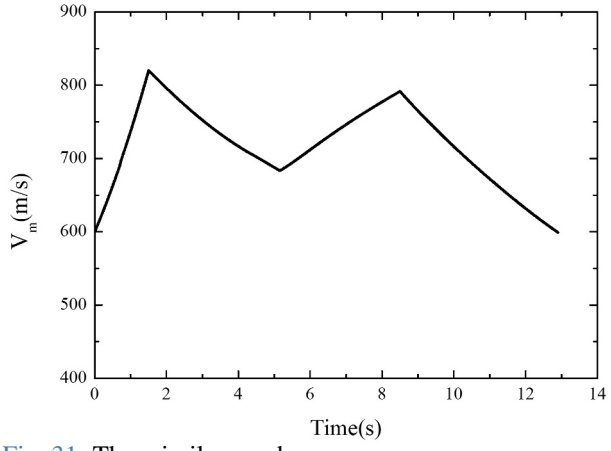

Fig. 31. The missile speed.

pared with the drag. When the thrust is less than the drag on the missile, the speed of the missile decreases.

5. CONCLUSIONS

In this paper, we have described the design of a new adaptive NFTSM guidance law for the missile intercepting the maneuvering target with impact angle constraints. The main characteristic of this design is that it combines the proposed novel nonsingular fast terminal sliding manifold and the adaptive algorithm. The proposed fast nonsingular terminal sliding manifold can solve the singularity problem and improve the convergence rate when the

guidance system state is far away from the equilibrium point. The adaptive approach is used to estimate the upper bound of lumped disturbance. With the proposed guidance law, a finite time convergence of the guidance system states in both the reaching phase and the sliding phase is guaranteed. Firstly, the simulation results for the constant speed missile show that the designed guidance law can guarantee that the LOS angle error and the LOS angular rate converge to small enough neighbourhoods around zero in finite time, respectively. And the proposed guidance law is robust against the target acceleration as an unknown bounded external disturbance and has highly precision guidance performance. Then, in order to illustrate the effectiveness of the proposed guidance law further, simulations for the realistic missile with varying speeds intercepting the maneuvering target with impact angle constraints, are performed.

REFERENCES

[1] S. Rogers, "Missile guidance comparison," *Proc. of the AIAA Conference on Guidance, Navigation, and Control*, pp. 1-4, 2004. [click]

[2] A. Ratnoo and D. Ghose, "Impact angle constrained interception of stationary targets," *Journal of Guidance, Control, and Dynamics*, vol. 31, no. 6, pp. 1817-1822, November-December 2008.[click]

[3] K. S. Erer and O. Merttopcuoglu, "Indirect impact-angle-control against stationary targets using biased pure proportional navigation," *Journal of Guidance, Control, and Dynamics*, vol. 35, no. 2, pp. 700-704, March-April 2012. [click]

[4] C. H. Lee, T. H. Kim, and M. J. Tahk, "Interception angle control guidance using proportional navigation with error feedback," *Journal of Guidance, Control, and Dynamics*, vol. 36, no. 5, pp. 1556-1561, September-October 2013. [click]

[5] D. Zhou, S. Sun, and K. L. Teo, "Guidance laws with finite time convergence," *Journal of Guidance, Control, and Dynamics*, vol. 32, no. 6, pp. 1838-1846, November-December 2009. [click]

[6] C. D. Yang and H. Y. Chen, "Nonlinear H_∞ robust guidance law for homing missiles," *Journal of Guidance, Control, and Dynamics*, vol. 21, no. 6, pp. 882-890, November-December 1998. [click]

[7] D. Zhou, C. D. Mu, and T. L. Shen, "Robust guidance law with L_2 gain performance," *Transactions of the Japan Society for Aeronautical and Space Sciences*, vol. 44, no. 144, pp. 82-88, August 2001. [click]

[8] W. H. Chen, J. L. Speyer, and D. Lianos, "Optimal intercept missile guidance strategies with autopilot lag," *Journal of Guidance, Control, and Dynamics*, vol. 33, no. 4, pp. 1264-1272, July-August 2010. [click]

[9] V. Shaferman and T. Shima, "Linear quadratic guidance law for imposing a terminal intercept angle," *Journal of Guidance, Control, and Dynamics*, vol. 31, no. 5, pp. 1400-1412, September-October 2008. [click]

[10] S. Sun, D. Zhou, and W. T. Hou, "A guidance law with finite time convergence accounting for autopilot lag," *Aerospace Science and Technology*, vol. 25, pp. 132-137, March 2013. [click]

[11] S. D. Brierley and R. Longchamp, "Application of sliding-mode control to air-air interception problem," *IEEE Transactions on Aerospace and Electronic Systems*, vol. 26, no. 2, pp. 306-325, March 1990. [click]

[12] Y. X. Zhang, M. W. Sun, and Z. Q. Chen, "Finite-time convergent guidance law with impact angle constraint based on sliding-mode control," *Nonlinear Dynamics*, vol. 70, no. 1, pp. 619-625, October 2012. [click]

[13] N. Harl and S. N. Balakrishnan, "Impact time and angle guidance with sliding mode control," *IEEE Transactions on Control Systems Technology*, vol. 20, no. 6, pp. 1436-1449, November 2012. [click]

[14] T. Yamasaki, S. N. Balakrishnan, and H. Takano, "Second order sliding mode-based intercept guidance with uncertainty and disturbance compensation," *Proc. of the AIAA Conference on Gudiance, Navigation, and Control*, pp. 19-22, 2013. [click]

[15] S. Rao and D. Ghose, "Sliding mode control based terminal impact angle constrained guidance laws using dual sliding surfaces," *Proc. of IEEE Workshop on Variable Structure Systems*, pp. 325-330, January 2012. [click]

[16] S. R. Kumar, S. Rao, and D. Ghose, "Sliding-mode guidance and control for all-Aspect interceptors with terminal angle constraints," *Journal of Guidance, Control, and Dynamics*, vol. 35, no. 4, pp. 1230-1246, July-August 2012. [click]

[17] Y. B. Shtessel, I. A. Shkolnikov, and A. Levant, "Guidance and control of missile interceptor using second-order sliding modes," *IEEE Transactions on Aerospace and Electronic Systems*, vol. 45, no. 1, pp. 110-124, January 2009. [click]

[18] Z. Man, A. P. Paplinski, and H. R. Wu, "A robust MIMO terminal sliding mode control scheme for rigid robotic manipulatiors," *IEEE Transactions on Automatic Control*, vol. 39, no. 12, pp. 2464-2469, December 1994. [click]

[19] Y. Feng, X. H. Yu, and Z. H. Man, "Non-singular terminal sliding mode control of rigid manipulators," *Automatica*, vol. 38, no. 12, pp. 2159-2167, December 2002. [click]

[20] L. Y. Wang, T. Y. Chai, and L. F. Zhai, "Neural-network-based terminal sliding mode control of robotic manipulators including actuator dynamics," *IEEE Transactions on Industrial Electronics*, vol. 56, no. 9, pp. 3296-3304, September 2009. [click]

[21] S. R. Kumar, S. Rao, and D. Ghose, "Non-singular terminal sliding mode guidance and control with terminal angle constraints for non-maneuvering targets," *Proc. of IEEE Workshop on Variable Structure Systems*, pp. 291-296, January 2012. [click]

[22] Q. Z. Song, X. Y. Meng, "Design and simulation of guidance law with angular constraint based on non-singular terminal sliding mode," *Physics Procedia*, vol. 25, pp. 1197-1204, April 2012. [click]

[23] S. R. Kumar, S. Rao, and D. Ghose, "Nonsingular terminal sliding mode guidance with impact angle constraints," *Journal of Guidance, Control, and Dynamics*, vol. 37, no. 4, pp. 1114-1130, July-August 2014. [click]

[24] S. F. Xiong, W. H. Wang, X. D. Liu, S. Wang, and Z. Chen, "Guidance law against maneuvering targets with intercept angle constraint," *ISA Transactions*, vol. 53, no. 4, July 2014. [click]

[25] X. H. Yu and Z. H. Man, "Fast terminal sliding mode control design for nonlinear dynamical systems," *IEEE Transactions on Circuits Systems Part I*, vol. 39, no. 2, pp. 261-264, February 2002. [click]

[26] S. H. Yu, X. H. Yu, and B. Shirinzadeh, "Continuous finite-time control for robotic manipulators with terminal sliding mode," Automatica, vol. 41, no. 11, pp. 1957-1964, November 2005. [click]

[27] Y. J. Huang, T. C. Kuo, and S. H. Chang, "Adaptive sliding-mode control for nonlinear systems with uncertain parameters," *IEEE Transactions on Systems, Man, and Cybernetics*, vol. 38, no. 2, pp. 534-539, April 2008. [click]

[28] B. L. Cong, C. Zhen, and X. D. Liu, "Disturbance observer-based adaptive integral sliding mode control for rigid spacecraft attitude maneuvers," *Proc. of the Institution of Mechanical Engineers, Part G: Journal of Aerospace Engineering*, vol. 227, no. 10, pp. 1660-1671, September 2013. [click]

[29] Z. Zhu, Y. Q. Xia, and M. Y. Fu, "Adaptive sliding mode control for attitude stabilization with actuator saturation," *IEEE Transactions on Industrial Electronics*, vol. 58, no. 10, pp. 4898–4907, 2011. [click]

[30] M. C. Pai, "Observer-based adaptive sliding mode control for robust tracking and model following," *International Journal of Control, Automation and Systems*, vol. 11, no. 2, pp. 225-232, October 2013. [click]

[31] C. Lu, X. Q. Chen, and S. Tao, "Fault tolerant small satellite attitude control using adaptive non-singular terminal sliding mode," *Advances in Space Research*, vol. 51, no. 12, pp. 2374-2393, June 2013. [click]

[32] B. Xiao, Q. L. Hu, and Y. M. Zhang, "Adaptive sliding mode fault tolerant attitude tracking control for flexible spacecraft under actuator saturation," *IEEE Transactions on Control Systems Technology*, vol. 20, no. 6, pp. 1605-1612, November 2012. [click]

[33] X. D. Liu, Y. J. Wu, and B. T. Liu, "The research of adaptive sliding mode controller for motor servo system using fuzzy upper bound on disturbances," *International Journal of Control, Automation and Systems*, vol. 10, no. 5, pp. 1064-1069, October 2012. [click]

[34] S. Frikha, M. Djemel, and N. Derbel, "Observer based adaptive neuro-sliding mode control for MIMO nonlinear systems," *International Journal of Control, Automation and Systems*, vol. 8, no.2, pp. 257-265, April 2010. [click]

[35] B. S. Kim, J. G. Lee, and H. S. Han, "Biased PNC law for impact with angular constraint," *IEEE Transactions on Aerospace and Electronic Systems*, vol. 34, no. 1, pp. 277-288, January1998. [click]

[36] T. Yamasaki, S. N. Balakrishnan, H. Takano, et al, "Second order sliding mode-based intercept guidance with uncertainty and disturbance compensation," *Proc. of AIAA Guidance, Navigation, and Control (GNC) Conference*, August 2013. [click]

[37] X. H. Wang, J. A. Wang, "Partial integrated guidance and control for missiles with three-dimensional impact angle constraints," *Journal of Guidance, Control, and Dynamics*, vol. 37, no. 2, pp. 644-657, March-April 2014. [click]

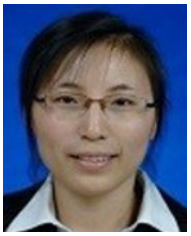

Junhong Song received her M.S. degree in Applied Mathematics from Harbin Institute of Technology in 2012. She is pursuing her Ph.D. degree at the School of Astronautics, Harbin Institute of Technology. Her main research interests include vehicle guidance and control.

Shenmin Song received his Ph.D. degree in Control Theory and Application from Harbin Institute of Technology in 1996. He carried out postdoctoral research at Tokyo University from 2000 to 2002. He is currently a professor at the School of Astronautics, Harbin Institute of Technology. His main research interests include spacecraft guidance and control, intelligent control, and nonlinear theory and application.

Huibo Zhou received her M.S. degree in College of Mathematics Normal Systems Science from Shenyang Normal University in 2006. Now she is a teacher at the School of Mathematical Science in Harbin Normal University, and at the same time she is pursuing her Ph.D. degree at the Center for Control Theory and Guidance Technology in Harbin Institute of Technology. Her main research interests include vehicle guidance and control.